$=1$ and $e^2=\alpha=1/137$. The Dirac matrices are defined as $\vec{\gamma}=-i\beta\vec{\alpha}$ and $\gamma_4=\beta$; $\gamma_5=\gamma_1\gamma_2\gamma_3\gamma_4$ and $\bar{\phi}=\phi^\dagger\gamma_4$.

[13]Glauber and Martin, Ref. 11, especially Sec. 6.

[14]See, for example, (29a) of I.

[15]Intemann, Ref. 10, Sec. III.

[16]Although it is not obvious from a direct comparison that (23) of this paper (in the limit: $f_o f_\delta^* \to 0$; $f_e \to I_e$) and (41) of I are equivalent, numerical evaluation of the two expressions demonstrates that indeed they are. The difference in form of the two results arises from the use of different representations for the ejected electron wave function.

[17]Of course the nuclear polarization $\mathcal{P}_M$ must also be determined by measuring the temperature or some other suitable property of the system.

[18]The result of this paper for the spectrum, while an improvement on the result of I, is not as accurate as the result obtained in II. In fact the result of II is found to deviate from the result of I by a little less than does the present result.

PHYSICAL REVIEW C VOLUME 6, NUMBER 1 JULY 1972

Hartree-Fock Calculations for Double-Closed-Shell Nuclei Using the Modified Delta Interaction*

Jerry W. Ehlers† and Steven A. Moszkowski
University of California at Los Angeles, Los Angeles, California 90024

(Received 2 March 1972)

Properties of double-closed-shell nuclei are calculated using the Hartree-Fock method. The effective nucleon-nucleon interaction is taken to be the density-dependent "modified δ interaction," which is closely related to the Skyrme interaction, but with only three free parameters. These parameters were chosen so as to reproduce, as well as possible, the binding energy and rms charge radii of ^{16}O and ^{208}Pb. This interaction leads to a binding energy 16.5 MeV/A and Fermi momentum 1.33 fm^{-1} of nuclear matter. Good agreement is found with the empirical rms charge radii of the other double-closed-shell nuclei, ^{40}Ca, ^{48}Ca, and ^{90}Zr. The same holds for the single-particle removal energies, especially those from $1s$ levels. The Hartree-Fock calculations with the present spin-independent and s-state interaction leads to as good agreement with experiment as those made by others, in particular, those made by Vautherin and Brink, who used a Skyrme interaction with five parameters.

The differences between the Skyrme and modified δ interaction are discussed. It is pointed out that the effective mass of a nucleon depends strongly on the odd-state part of the interaction, while the asymmetry potential is also sensitive to its spin dependence.

1. INTRODUCTION

Recently some nuclear-structure calculations have been made by several authors using simplified forces such as the interaction developed by Skyrme.[1] One such interaction, the modified δ interaction (MDI) developed by one of us,[2] contains just three parameters. The purpose here is to extend to finite nuclei the studies of the MDI which have already been done with the hypothetical semi-infinite nuclear-matter model.

The MDI[2] is a simple effective interaction of the form

$$V(\vec{r}_1,\vec{r}_2)=V(\vec{r},\vec{s})=-\alpha\delta(\vec{s})+\tfrac{1}{2}\beta[k^2\delta(\vec{s})+\delta(\vec{s})k^2]+\gamma(\tfrac{3}{2}\pi^2)^{2/3}\rho^{2/3}(\vec{r})\delta(\vec{s}), \quad (1)$$

where

$\vec{s}=\vec{r}_1-\vec{r}_2$,

$\vec{k}=$ momentum operator,

$\vec{r}=\frac{1}{2}(\vec{r}_1+\vec{r}_2)$,

$\rho(\vec{r})=$ total matter density at $\vec{r}$.

The factor $(\frac{3}{2}\pi^2)^{2/3}$ is introduced so that the last term has a coefficient $\gamma k_f^2(r)$, where $k_f(r)$ is the local Fermi momentum. For equal neutron and proton densities the total nuclear energy can be written explicitly in terms of the total mass density (ρ) and kinetic energy density (τ) (ignoring Coulomb energies and c.m. corrections). Further details are given in Ref. 2. Recently, Vautherin and Brink (VB)[3] made calculations similar to some of those reported in this paper using the full Skyrme interaction, which contains two more parameters than ours – namely a spin dependence and an odd-state interaction. However, as will be seen, our interaction fits bound-state experimental quantities practically as well as theirs.

2. SINGLE-PARTICLE POTENTIAL

With the MDI, the Hartree-Fock (HF) problem is greatly simplified. The HF single-particle self-consistent potential can simply be expressed in terms of the total density ρ and the kinetic energy

density τ (Appendix I). For identical neutron and proton densities

$$U_{\mathrm{HF}}(\vec{r}) = -\tfrac{3}{4}\alpha\rho - \tfrac{9}{64}\beta\nabla^2\rho - \tfrac{3}{32}\beta(\nabla^2\cdot\rho + \rho\nabla^2) + \tfrac{3}{16}\beta\tau + \tfrac{3}{4}\gamma(\tfrac{3}{2}\pi^2)^{2/3}\rho^{5/3}. \quad (2)$$

The expression $\nabla^2\cdot\rho$ is understood to mean that ∇^2 acts on *all* terms to its right. Thus, the contribution of $\nabla^2\cdot\rho$ to $U_{\mathrm{HF}}\psi$ is $\nabla^2(\rho\psi)$. However, in the present calculations allowance was made for nonidentical neutron and proton densities. The HF potential for neutrons can thus be written as follows:

$$U_{\mathrm{HF},n} = -\alpha(\tfrac{1}{2}\rho_n + \rho_p) - \tfrac{3}{16}\beta(\tfrac{1}{2}\nabla^2\rho_n + \nabla^2\rho_p) - \frac{\hbar^2}{4M}(\nabla^2\cdot W_n + W_n\nabla^2) + \tfrac{1}{4}\beta(\tfrac{1}{2}\tau_n + \tau_p) + \gamma(\tfrac{3}{2}\pi^2)^{2/3}\rho^{2/3}(\tfrac{1}{2}\rho_n + \rho_p), \quad (3)$$

where

$$W_n = \frac{1}{4}\frac{2M}{\hbar^2}\beta(\tfrac{1}{2}\rho_n + \rho_p),$$

$$\rho = \rho_n + \rho_p,$$

$$\tau = \tau_n + \tau_p.$$

To obtain the proton potential (apart from Coulomb effects) we merely interchange n and p everywhere.

A further difference between the potentials is the Coulomb force in the potential of the protons. The direct Coulomb potential is calculated from the proton density, while the exchange part of the Coulomb interaction in the potential is ignored because of its complexity and its insignificance. However, the energy due to the Coulomb-exchange interaction is calculated by using the constant-density approximation as derived by Bethe and Bacher,[4] and is then added into the final total energy.

The MDI is purely an s-wave interaction, and thus has no two-body spin-orbit coupling force. Therefore, in order to fill up the particles in the proper energy levels, one was artificially included in the single-particle spin-orbit coupling potential as the derivative of the total density[5]:

$$U_{ls} = U_{ls0}\frac{1}{r}\frac{d}{dr}\rho. \quad (4)$$

Vautherin and Veneroni[6] had used this same expression in their calculations with a strength constant of $U_{ls0} = 176$ MeV fm^5 as determined from the energy splitting of the p shell in ^{16}O (actually from the experimental excitation energies of ^{15}N).

The single-particle Hamiltonian is the same regardless of whether the single-particle potential is due to one-body or two-body forces (and consequently the eigenvalues are unaffected); however, the total energy is affected. It is therefore assumed that the approximation of the spin-orbit single-particle potential is due entirely to two-body density-independent forces, for example, spin-orbit and tensor forces. Having the potential due to two-body forces enables the total energy to be treated the same as the HF potential:

$$E = \tfrac{1}{2}\sum_i[(\hbar^2/2M)\langle\tau_i\rangle + E_i] \quad (5)$$

instead of

$$E = \sum_i(\hbar^2/2M)\langle\tau_i\rangle + \tfrac{1}{2}\sum_i\sum_j\langle V_{ij}\rangle + \sum_i\langle V_{ls}\rangle_i. \quad (6)$$

In dealing with a density-dependent interaction, when a particle is added to the nucleus, thus altering the total density, the single-particle potential is changed. This change is called the rearrangement potential, and it is added to the HF single-particle potential. The energy due to the rearrangement potential is eventually subtracted off to give the total HF energy.[7,8] In order to keep the total energy minimized within the framework of the HF theory, the significant part of the rearrangement potential is[7]

$$\langle i|U_R|i\rangle = \frac{1}{2}\sum_j\sum_\alpha\left\langle j\alpha\left|\psi_i^*\psi_i\frac{\partial V}{\partial\rho}\right|j\alpha\right\rangle. \quad (7)$$

Since the density-dependent part of the MDI is proportional to $\rho^{2/3}(r)$, the rearrangement potential is (Appendix II)

$$U_R(r) = \tfrac{1}{6}(\tfrac{3}{2}\pi^2)^{2/3}\gamma(\rho_p^2 + 4\rho_p\rho_n + \rho_n^2)\rho^{-1/3}, \quad (8)$$

and for $N = Z$ this expression reduces to

$$U_R(r) = \tfrac{1}{4}(\tfrac{3}{2}\pi^2)^{2/3}\gamma\rho^{5/3} \quad (9)$$

which has to be added to the HF potential (2) to obtain the total single-particle potential.

3. TREATMENT OF NONLOCAL POTENTIAL

The single-particle potential (including rearrangement, Coulomb corrections, and spin-orbit coupling) is nonlocal (unless $\beta = 0$). It can be expressed in the form

$$U(r) = V(r) - \frac{\hbar^2}{4M}[\nabla^2\cdot W(r) + W(r)\nabla^2]. \quad (10)$$

It was shown by Green[9] that this potential can be transformed into a local one. The original single-particle wave function is ψ_i. Now define a new wave function

$$\phi_i = (1+W)^{1/2}\psi_i. \quad (11)$$

Then ϕ_i is the solution of a new Schrödinger equation with a local potential[9]

$$U^{\mathrm{eff}} = \frac{V + WE}{1+W} - \frac{1}{4}\left(\frac{dW/dr}{1+W}\right)^2. \quad (12)$$

An alternative approach was followed in the present work. The nonlocal Schrödinger equation was transformed without a modification of the wave function. This gives a Schrödinger-like equation of the form

$$\nabla^2\psi_i+\frac{dW/dr}{1+W}\frac{d\psi_i}{dr}+\frac{E_i-V+(\hbar^2/4M)\nabla^2 W}{1+W}\psi_i=0. \quad (13)$$

Once the wave functions are obtained, the particle density and kinetic energy density for neutrons are given by the following expressions

$$\rho_n=\sum_n\sum_l\sum_j\frac{2j+1}{4\pi}u^2, \quad (14a)$$

$$\tau_n=\sum_n\sum_l\sum_j\frac{2j+1}{8\pi}\left[\nabla(u^2)-u\nabla^2u+\frac{2l(l+1)u^2}{r^2}\right], \quad (14b)$$

where u denotes radial wave functions: $u=u_{nlj}(r)$. Similar expressions are obtained for protons.

4. CENTER-OF-MASS AND PROTON-SIZE CORRECTIONS

In addition to the c.m. correction, the size of each proton must be considered to calculate the rms radius of the charge distribution ($\langle r^2\rangle_{\rm ch}^{1/2}$) from the rms radius of the proton-matter density[2]:

$$\langle r^2\rangle_{\rm ch}=\langle r^2\rangle_{\rm prot.\ matt.}+\langle r^2\rangle_{\rm prot.}-\frac{3}{2}\frac{b_p^2}{A}, \quad (15)$$

where b_p is an oscillator length related to the proton-matter radius by

$$\langle r^2\rangle_{\rm prot.\ matt.}=\frac{b_p^2\sum_i(N_i+\frac{3}{2})(2j_i+1)}{\sum_i(2j_i+1)}. \quad (16)$$

The experimental rms radius of the proton, $\langle r^2\rangle_{\rm prot.}^{1/2}$, is 0.8 fm.

In a paper by Negele[10] it is shown that the c.m. correction and finite size of the proton can be incorporated into an integral for the calculation of the charge distribution from the proton-mass density:

$$\rho_{\rm ch}(\vec{r})=\int d^3r_1[(P^2-B^2)\pi]^{-3/2}\times\exp\left[-\frac{(\vec{r}-\vec{r}_1)^2}{P^2-B^2}\right]\rho_{\rm HF}^p(\vec{r}_1), \quad (17)$$

where

$$B^2=b_p^2/A, \quad P^2=\tfrac{3}{2}\langle r^2\rangle_{\rm prot.}.$$

When the HF proton density is spherically symmetric, the charge distribution can be expressed as a single integral of the form

$$\rho_{\rm ch}(r)=\frac{[\pi(P^2-B^2)]^{-1/2}}{r}\int r_1dr_1\left\{\exp\left[-\frac{(r-r_1)^2}{P^2-B^2}\right]-\exp\left[-\frac{(r+r_1)^2}{P^2-B^2}\right]\right\}\rho_{\rm HF}^p(r_1). \quad (18)$$

The total energy is

$$E=\tfrac{1}{2}\sum_i[(\hbar^2/2M)\langle\tau_i\rangle+E_i]-\tfrac{1}{2}E_R+E_x-E_{\rm c.m.}, \quad (19)$$

where

$$E_R=\int\rho(\vec{r})U_R(\vec{r})d^3r,$$

$$E_x=-\left(\frac{243}{256\pi^2}\right)^{1/3}\frac{e^2Z^{4/3}}{R_{\rm eff}},$$

$$R_{\rm eff}=(\tfrac{5}{3}\langle r^2\rangle_{\rm prot.\ matt.})^{1/2},$$

$$E_{\rm c.m.}=\frac{3}{4}\left(\frac{Z}{A}\hbar\omega_p+\frac{N}{A}\hbar\omega_n\right),$$

$$\hbar\omega_p=\hbar^2/Mb_p^2,$$

$$\hbar\omega_n=\hbar^2/Mb_n^2.$$

5. MDI PARAMETERS

In Ref. 2, the MDI parameters were taken so as to reproduce the value $k_F=1.36$ fm^{-1} for the Fermi momentum of nuclear matter [and also 15.75 MeV per particle for the volume binding energy of nuclear matter and 7.98 MeV for the binding energy per particle of ^{16}O in the harmonic-oscillator (HO) approximation]. This value for k_F is determined from electron scattering cross sections from ^{208}Pb under the assumption that the neutrons and protons occupy the same volume. This assumption was made by Elton,[11] who tabulated the resultant maximum densities obtained from electron scattering cross sections assuming a Fermi distribution. The central charge density is 0.067 per fm^3. The proton density is the same, and under the above assumption, the total nucleon density is 0.170 nucleons/fm^3 and $k_F=1.36$ fm^{-1}.

Our new parameters are obtained by fitting the binding energy (7.87 MeV per nucleon) and rms radius (5.51 fm) of ^{208}Pb and the binding energy (7.98 MeV per nucleon) of ^{16}O using the HF method. The new MDI parameters are:

$$\alpha=1244.4\ \text{MeV fm}^3,\quad \beta=646.4\ \text{MeV fm}^5,\quad \gamma=144.7\ \text{MeV fm}^5. \quad (20)$$

This interaction gives a nuclear-matter binding energy of 16.46 MeV per nucleon and a Fermi momentum 1.33 fm^{-1}, i.e., a Fermi kinetic energy of 36.7 MeV. The difference in the two Fermi mo-

menta can be understood as follows: The assumption that the neutron and proton distributions have the same radius is unjustified. The results of our calculations, shown in Table II, indicate that in ^{208}Pb the neutron rms radius exceeds the rms radius of the protons by 0.19 fm. Similar results were obtained by others.[3,10]

The rms radius of the matter distribution, both protons and neutrons, exceeds the rms proton radius by 0.12 fm, that is, by 2.2%. Because of this difference, the total nucleon density is smaller than under our previous assumptions by 6.5%; thus $\rho_0 = 0.159/\text{fm}^{-3}$ and $k_F = 1.33\ \text{fm}^{-1}$.

It should be mentioned here that the "old" MDI gave a surface energy of semi-infinite nuclear matter of 19.3 MeV, and a 90 to 10% surface thickness of 2.2 fm. For the "new" MDI used here these two quantities are increased to 21.2 MeV and 2.6 fm, respectively.

6. NUCLEAR MATTER FOR MDI

Before discussing the results of our HF calculation, let us remark on some properties of nuclear matter obtained with the MDI; namely the effective mass, the asymmetry energy, and the asymmetry (isovector) potential.

For an MDI and, more generally, for the Skyrme interaction, the single-particle potential is a quadratic function of momentum, a linear function of the energy. This is, of course, a defect of the MDI and Skyrme interactions. Both experiment[12] and calculations using realistic nucleon-nucleon interactions[13] lead to decreased energy dependence of the potential with increasing energy. In any case, we obtain

$$\frac{m}{m^*} = 1 + \frac{3}{16}\,\frac{2M}{\hbar^2}\,\beta\rho\,. \tag{21}$$

With our parameters we obtain an effective mass of $0.51m$, considerably lower than the value $0.6m$, as an average effective mass over the Fermi sea, and 0.7 to $1.1m$ for the most loosely bound nucleons.[14]

Also the real part of the isoscalar potential (average of proton and neutron potentials, excluding the Coulomb term) in nuclear matter is too weak,

$$U_0 = 46 - 0.5E\,, \tag{22}$$

compared with the empirical form[15]:

$$U_0 = 55 - 0.32E\,. \tag{23}$$

The asymmetry energy of nuclear matter is

$$c_\tau = \tfrac{1}{3}T_F + \tfrac{1}{8}\rho(\alpha - \gamma k_F{}^2) = 31.9\ \text{MeV} \tag{24}$$

with our values of the parameters, in good agreement with other estimates of this quantity, both from known nuclear binding energies[16] and from calculations using more realistic interactions.[17] On the other hand, the asymmetry (i.e., isovector) potential of nuclear matter [the coefficient of $(N-Z)/A$] is given by[18]

$$U_1 = 2c_\tau - \tfrac{2}{3}(m/m^*)T_F\,, \tag{25}$$

which is only 16 MeV with our parameters, compared with an empirical value of about 24 MeV from optical-model analyses.[15]

The calculated isovector potential, like the depth of the isoscalar potential U_0, is expected to decrease with energy, in particular $\frac{1}{3}$ as fast as U_0. This increases the discrepancy slightly, i.e., for a nucleon of zero energy, we find $U_1 = 14$ MeV. However, the anomalous proton-potential term (which is due to the momentum dependence of the optical potential) is

$$U_A = \frac{6}{5}\,\frac{Ze^2}{R}\left(1 - \frac{m^*}{m}\right) \sim \frac{0.7Z}{A^{1/3}} \tag{26}$$

for our set of parameters and $R = 1.2\,A^{1/3}$. The empirical value of this coefficient is well known to be about 0.4.[19] It is interesting to note that for the proton single-particle potential, the discrepancy between isovector and anomalous Coulomb terms largely cancels.[20] For nuclei on the β-stability line we have, according to the conventional semiempirical binding-energy formula

$$Z/A^{1/3} = 65(N-Z)/A\,. \tag{27}$$

Thus, our calculated sum is

$$U_1 + U_A = 60(N-Z)/A \tag{28}$$

compared with an empirical value 50 MeV for the coefficient.

Of course, for neutron scattering and quasielastic (n,p) charge exchange, the anomalous Coulomb term does not appear and the discrepancy is much larger. This discrepancy, can however, be removed by making the interaction, in particular the α term, spin-dependent. We have

$$V_\alpha = -(1 + x_0 P_\sigma)\alpha\,\delta(\vec{s})\,, \tag{29}$$

where P_σ is the spin-exchange operator. Some such spin dependence with $x_0 > 0$ is expected to occur from simple Boson-exchange models and is well known to be required to account for the spectra of odd-odd nuclei. This spin dependence has no effect on nuclear matter and for $N = Z$ nuclei. However, for neutron-rich nuclei, the binding energy is lowered. More specifically, the asymmetry energy is increased by an amount

$$\Delta c_\tau = \tfrac{1}{4}\rho x_0 \alpha\,. \tag{30}$$

TABLE I. Binding energy per nucleon (MeV) of double-closed-shell nuclei for the MDI using the new MDI parameters, compared with experimental, Németh-Vautherin (NV, Ref. 21), Vautherin-Brink (VB, Ref. 3, interaction II), Negele [N, Ref. 10, revised values (see H. A. Bethe, Ref. 36)] and Köhler (K, Ref. 22, Model D1), and Miller-Green (MG, Ref. 23).

Nucleus	^{16}O	^{40}Ca	^{48}Ca	^{90}Zr	^{208}Pb
MDI	7.98	8.67	8.45	8.63	7.88
NV	7.73	8.32	7.87	8.07	7.31
VB	7.89	8.41	8.39	8.43	7.54
N	7.59	7.99	7.96	8.33	7.83
K	7.93	8.53	8.67	8.75	8.01
MG	7.35	8.25	8.55	8.87	8.05
Expt	7.98	8.55	8.67	8.71	7.87

For

$$x_0 = 0.1\,, \quad \Delta c_\tau = 5 \text{ MeV}$$

and, for example, the binding energy per particle of ^{208}Pb is reduced by 0.13 MeV, a very small amount. On the other hand, the isovector potential in nuclear matter is increased by $2c_\tau = 10$ to 26 MeV, in good agreement with the experimental value in finite nuclei.

7. HF CALCULATIONS-RESULTS

In the HF calculation, good agreement with experimental binding energies and charge radii was obtained with the MDI. Our value of $k_F = 1.33$ fm^{-1} is quite close to the value that VB[3] get from their Skyrme-interaction calculations ($k_F = 1.30$ or 1.32 fm^{-1}), and the value 1.31 fm^{-1} obtained by Negele.[10] The results for the MDI are given in the tables. These are compared with the results obtained by VB[3] (force II); Negele[10]; Németh and Vautherin,[21] who used a modification of Negele's interaction; Köhler[22] (interaction D), who used a density-dependent effective interaction somewhat more complicated than ours and Skyrme's; and Miller and Green,[23] who used a relativistic one-boson-exchange interaction; and, finally, the experimental results. Experimental binding energies were taken from the Atomic Mass Table of Mattauch, Thiele, and Wapstra[24]; and charge rms radii were taken from Collard, Elton, and Hofstadter[25] and from Ref. 3.

TABLE II. rms radii of neutron (neut), proton (prot), charge (ch), and matter densities (matt) (in fm) for the MDI.

Nucleus	^{16}O	^{40}Ca	^{48}Ca	^{90}Zr	^{208}Pb
$r_{\rm rms}$ (neut)	2.56	3.29	3.61	4.28	5.64
$r_{\rm rms}$ (prot)	2.58	3.35	3.42	4.19	5.45
$r_{\rm rms}$ (ch)	2.71	3.44	3.51	4.27	5.51
$r_{\rm rms}$ (matt)	2.57	3.32	3.53	4.24	5.57

TABLE III. rms radii of the charge distributions (in fm). See further information in the caption of Table I.

Nucleus	^{16}O	^{40}Ca	^{48}Ca	^{90}Zr	^{208}Pb
MDI	2.71	3.44	3.51	4.27	5.51
NV	2.76	3.45	3.52	4.23	5.44
VB	2.75	3.49	3.54	4.31	5.55
N	2.83	3.50	3.54	4.26	5.50
K	2.81	3.60	3.68	4.47	5.76
MG	2.70	3.49	3.49	4.30	5.54
Expt	2.73	3.50	3.49	4.30	5.52

The binding energies per particle are given in Table I. The results are for the most part in good agreement with the experimental energies. This is much better than expected considering the simplicity of this interaction. The Skyrme interaction used by VB[3] is the next simplest interaction with an extra spin-dependent parameter and also an extra p-wave-interaction parameter which the MDI does not have. Their spin-orbit potential is also more involved for nonidentical neutron and proton densities than that used here.

We also calculated the binding energy in MeV per nucleon for several other nuclei. The empirical and calculated values are given here: ^{4}He (7.09, 6.66); ^{12}C (7.68, 6.06); ^{60}Ni (8.78, 8.15); ^{120}Sn (8.51, 8.50); ^{140}Ce (8.38, 8.39); $^{298}_{114}$X (?, 7.13). After taking into account the c.m. motion, the calculated rms radii of the total nucleon-matter densities and the densities of the protons, neutrons, and charge are given in Table II. In Table III, the rms of the charge distributions are compared with the experimental values and those calculated by various authors.

The neutron and proton separation energies are given in Tables IV and V, respectively. These energies are in as comparable agreement with experiment as the others.

The single-particle energy levels are given in Table VI for ^{16}O, ^{40}Ca, ^{48}Ca, ^{90}Zr, and ^{208}Pb using the MDI (new parameters). Empirical values

TABLE IV. Neutron separation energies (MeV) for double-closed-shell nuclei. See caption for Table I.

Nucleus	^{16}O	^{40}Ca	^{48}Ca	^{90}Zr	^{208}Pb
MDI	16.5	17.7	10.4	12.8	9.3
NV	14.8	15.5	8.0	...	7.6
VB	16.8	17.5	9.1	11.5	7.0
K	14	15	10	12	9.0
Expt	15.7	15.6	9.9	12.0	7.4

TABLE V. Proton separation energies (MeV) for double-closed-shell nuclei. See caption for Table I.

Nucleus	^{16}O	^{40}Ca	^{48}Ca	^{90}Zr	^{208}Pb
MDI	12.7	10.1	16.4	8.0	8.7
NV	11.3	8.6	15.5	···	8.8
VB	13.0	10.1	16.5	7.9	9.0
K	10	8	15	8	9
Expt	12.1	8.3	15.3	7.9	8.0

are listed in Ref. 3. Table VII lists the $1s_{1/2}$ proton single-particle energies calculated for the new MDI, compared with those obtained by various authors. Both our and VB's energies agree very well with experimental values.

The matter densities (without c.m. corrections) and charge distributions (in units of e, the charge per proton) are plotted for ^{16}O, ^{40}Ca, ^{48}Ca, ^{90}Zr, and ^{208}Pb in Figs. 1(a) to 1(e). Electron scattering has given much information on the charge distribution of various nuclei by adjusting parameters of assumed analytic shapes.[26] These densities are also plotted for ^{40}Ca, ^{48}Ca, and ^{208}Pb. These analytic densities, while quite accurate, do not reproduce the expected shell-structure oscillations. The elastic electron scattering cross sections for several double-closed-shell nuclei were calculated by several authors.[27] Excellent agreement with experimental cross sections was obtained by these groups. Their calculated HF charge densities are only slightly different from each other.

TABLE VI. Single-particle energies in double-closed-shell nuclei calculated with MDI compared with experimental values. (See Ref. 3.) Occupied and empty levels are separated by horizontal lines.

Level	Neutron MDI	Neutron Expt	Proton MDI	Proton Expt
		^{16}O		
$1s_{1/2}$	45.6		41.3	40 ± 8
$1p_{3/2}$	22.7	21.8	18.7	18.4
$1p_{1/2}$	16.5	15.7	12.7	12.1
$1d_{5/2}$	4.2	4.1	0.8	0.6
$2s_{1/2}$	1.6	3.3		
$1d_{3/2}$				
		^{40}Ca		
$1s_{1/2}$	62.2		53.6	50 ± 11
$1p_{3/2}$	42.8		34.7	34 ± 6
$1p_{1/2}$	39.0		30.8	
$1d_{5/2}$	24.5		16.8	
$2s_{1/2}$	18.0	18.1	10.4	10.9
$1d_{3/2}$	17.7	15.6	10.1	8.3
$1f_{7/2}$	8.0	8.4	0.9	1.4
		^{48}Ca		
$1s_{1/2}$	62.1		57.4	55 ± 9
$1p_{3/2}$	43.9		40.3	35 ± 7
$1p_{1/2}$	41.2		37.5	
$1d_{5/2}$	26.4		23.2	
$2s_{1/2}$	20.5	12.6	17.5	15.3
$1d_{3/2}$	20.7	12.5	16.4	15.7
$1f_{7/2}$	10.4	9.9	7.2	9.6
$2p_{3/2}$	5.1	5.1		
		^{90}Zr		
$1s_{1/2}$	70.2		58.9	54 ± 8
$1p_{3/2}$	56.2		46.0	43 ± 8
$1p_{1/2}$	54.6		44.4	
$1d_{5/2}$	41.4		32.1	27 ± 8
$1d_{3/2}$	38.0		28.5	
$2s_{1/2}$	36.0		25.7	
$1f_{7/2}$	26.8		17.9	
$1f_{5/2}$	21.0	13.5	12.1	
$2p_{3/2}$	19.9	13.1	10.0	
$2p_{1/2}$	17.8	12.6	8.0	
$1g_{9/2}$	12.8	12.0	4.2	
$1g_{7/2}$	5.0	7.2		
		^{208}Pb		
$1s_{1/2}$	72.1		58.2	
$1p_{3/2}$	63.7		50.2	
$1p_{1/2}$	63.1		49.6	
$1d_{5/2}$	54.2		41.0	
$1d_{3/2}$	53.0		39.6	
$2s_{1/2}$	50.4		38.5	
$1f_{7/2}$	43.9		30.9	
$1f_{5/2}$	41.6		28.3	
$2p_{3/2}$	38.1		24.2	
$2p_{1/2}$	36.9		23.0	
$1g_{9/2}$	33.0		20.2	15.4
$1g_{7/2}$	29.3		16.2	11.4
$2d_{5/2}$	25.8		12.0	9.7
$2d_{3/2}$	23.7		9.9	9.4
$1h_{11/2}$	21.9		9.2	8.4
$3s_{1/2}$	22.8		8.7	8.0
$1h_{9/2}$	16.5	10.8	3.5	3.8
$2f_{7/2}$	14.0	9.7	0.3	2.9
$2f_{5/2}$	11.1	8.0		
$1i_{13/2}$	11.0	9.0		
$3p_{3/2}$	10.4	8.3		
$3p_{1/2}$	9.3	7.4		
$1i_{11/2}$	3.9	3.2		
$2g_{9/2}$	3.1	3.9		

TABLE VII. Removal energies of 1s protons (MeV) for double-closed-shell nuclei. See caption for Table I.

Nucleus	^{16}O	^{40}Ca	^{48}Ca	^{90}Zr	^{208}Pb
MDI	41.3	53.6	57.4	58.9	58.2
NV	30.5	37.7	41.1		40.9
VB	38.0	47.1	53.2	52.7	53.4
N		46.9			
K	29	36	40	40	40
MG	38	48	55		53
Expt	40 ± 8	50 ± 11	55 ± 9	54 ± 8	···

8. ASYMMETRY EFFECTS

We have also calculated the isoscalar and isovector potentials for two neutron-rich double-closed-shell nuclei, ^{208}Pb and ^{48}Ca. Figure 2(a) shows the matter density, the neutron excess, and the isoscalar and isovector potentials, for nucleons on top of the Fermi sea, in ^{208}Pb. As is well known, the isoscalar potential extends significantly (0.5 fm) beyond the matter distribution (as determined, say, by the half-fall-off radii). As can be seen from the figure, the isovector potential extends about 0.7 fm beyond the isoscalar part. In that sense, the isovector potential is partially a surface effect,[28] even though there is no real surface peaking (in ^{208}Pb). Note, however, that the strength of the isovector potential is only about 14 MeV, much smaller than the experimental value and even slightly smaller than the calculated strength in nuclear matter (for MDI). As can be seen from the figure, the neutron excess in the nuclear interior is on the average about 20% less than the nuclear matter value, i.e., the ratio of neutron to proton densities is slightly less than N/Z. (This is, of course, compensated for by a larger neutron excess at the nuclear surface.)

We have already mentioned that the strength of the isovector potential is very sensitive to a spin dependence in the interaction. Thus, by using a

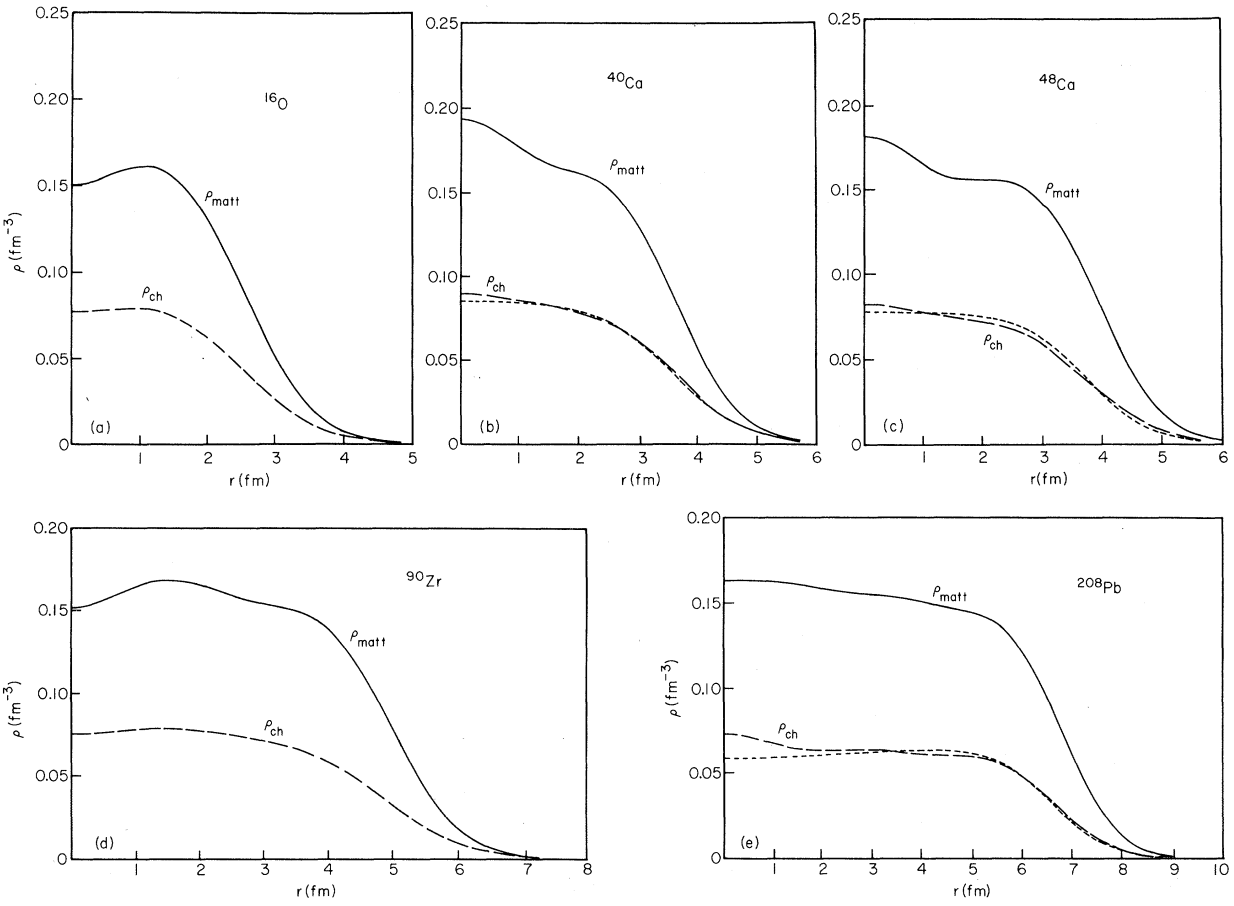

FIG. 1. Matter density (ρ_{matt}) and charge distribution (ρ_{ch}) for (a) ^{16}O, (b) ^{40}Ca, (c) ^{48}Ca, (d) ^{90}Zr, (e) ^{208}Pb for the modified δ interaction. For ^{40}Ca, ^{48}Ca, and ^{208}Pb, the empirical charge distribution is also shown by a short-dashed line.

spin-dependent δ interaction of the form (29) with $x_0 = 0.1$, the asymmetry potential is raised to about 22 MeV in the interior, close to the empirical value. There is an interesting effect here. In going from $x_0 = 0$ to $x_0 = 0.1$ (but keeping all other parameters of the MDI fixed), the rms radius of the neutron distribution increases from 5.64 to 5.67 fm. On the other hand, the proton rms radius remains at 5.46 fm.

Turning now to ^{48}Ca, as can be seen from Fig. 2(b), the isovector term not only extends outside the isoscalar potential, but it is strongly peaked at the nuclear surface. This occurs because the neutron excess (neutrons in the $f_{7/2}$ shell) is surface peaked.[29]

9. COMPARISON WITH RESULTS USING HO POTENTIAL

HF wave functions are expected to be more realistic than HO wave functions, thus resulting in correspondingly more binding energy per particle in going from the HO calculations, to the HF results. Table VIII shows this comparison for ^{16}O and ^{40}Ca (using the MDI parameters). The rms radii of the particle density are also given for ^{16}O and ^{40}Ca using the HO approximation and the HF method. These results show the consistency and validity of these methods, and also act as a check on the individual calculations. Figure 3 shows the particle densities for each of these two methods. Again these figures show the consistency of the methods in calculating the densities.

TABLE VIII. Comparison of binding energy per nucleon (MeV) and rms radius, ^{16}O and ^{40}Ca, of the charge density using the HO approximation and the HF, for MDI interaction.

Nucleus	^{16}O	^{40}Ca
E/A (HO)	7.86	8.42
E/A (HF)	7.98	8.67
$r_{\rm rms}$ (HO)	2.69	3.43
$r_{\rm rms}$ (HF)	2.71	3.44

10. VARIATION OF DENSITY DEPENDENCE OF MDI

The density dependence of the MDI used in this paper is contained in the $\rho^{2/3}$ term. However, it might be of interest to see if our results are greatly changed if one uses a slightly different

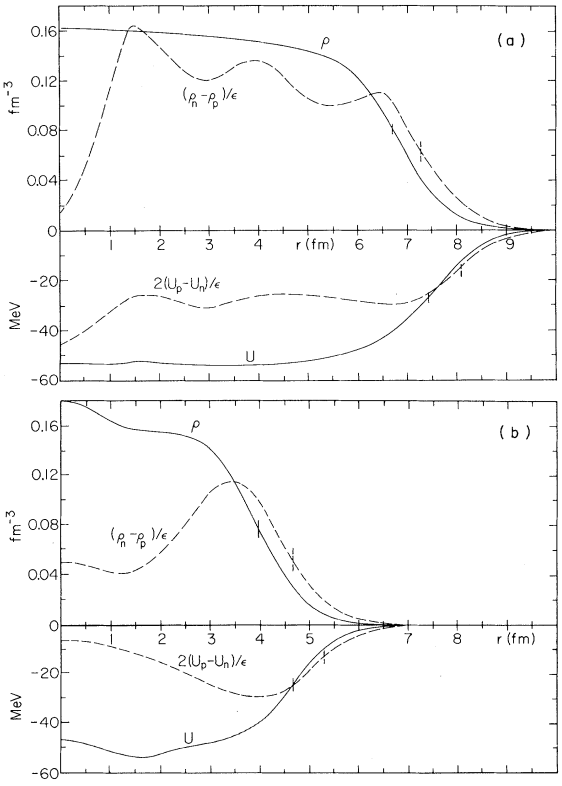

FIG. 2. Calculated matter density distribution ρ and fractional neutron excess $(\rho_n - \rho_p)/\epsilon$, compared with single-particle average potential U and asymmetry potential $(U_p - U_n)/\epsilon$, $\epsilon = (N-Z)/A$, for valence nucleons. The radii at which each of these quantities have fallen to half of their maximum values are indicated by short vertical lines: (a) for ^{208}Pb, (b) for ^{48}Ca.

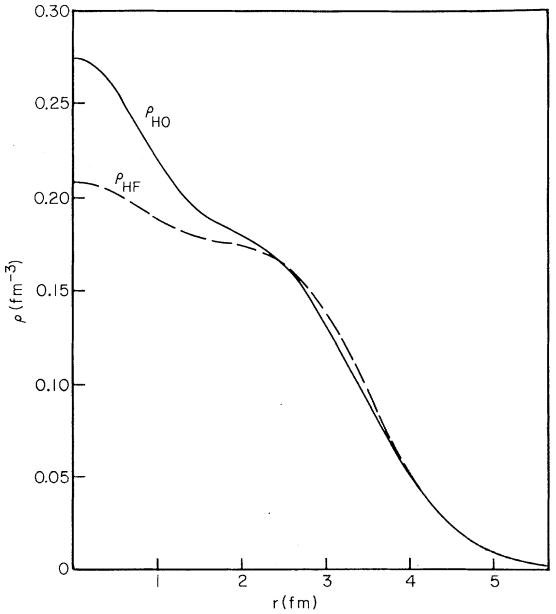

FIG. 3. Comparison of the matter densities in ^{40}Ca calculated using the harmonic-oscillator model ($\rho_{\rm HO}$) and the Hartree-Fock method ($\rho_{\rm HF}$) (using the MDI with parameters of Ref. 2).

density-dependent δ interaction. For example, the Skyrme interaction[1] has a slightly different implied density dependence, ρ^1. Such a density dependence may simplify some calculations of shell-model matrix elements.

To test this point we repeated some of the HF calculations using an MDI with a ρ^1 dependence

$$\gamma^1\left(\frac{3\pi^2}{2}\right)\rho(\vec{r})\delta(\vec{s}).$$

Matching the ^{208}Pb binding energy and rms charge radius, and the binding energy ^{16}O gave new parameters:

$$\alpha = 1169.2 \text{ MeV fm}^3, \quad \beta = 626.0 \text{ MeV fm}^5,$$
$$\gamma^1 = 81.7 \text{ MeV fm}^6. \tag{31}$$

The results for this interaction differ only very slightly from those obtained for the present MDI interaction. The binding energy and Fermi momentum of nuclear matter are 16.43 MeV/A and 1.32 fm^{-1}. For ^{40}Ca we obtain practically the same results as before. Similar conclusions are obtained for the single-particle energy levels and the charge distribution.

11. COMPARISON OF MDI AND SKYRME INTERACTION

The MDI interaction is essentially a simplified version of the interaction proposed by Skyrme. Let us briefly comment on the significant differences between these two interactions.

p-State Interaction

The MDI is assumed to act only in s states of relative motion, while the Skyrme interaction also contains a p-wave interaction of the form $-t_2\nabla\cdot\delta(\vec{s})\cdot\nabla$. However, in the recent VB calculation, the coefficient of the t_2 term is very small: −27 MeV fm^5 for "force II" (attractive) compared to about 600 MeV fm^5 for the s-wave term $-\frac{1}{2}t_1 \times[\delta(\vec{s})\nabla^2+\nabla^2\cdot\delta(\vec{s})]$. ($t_1$ = our β.)

Nevertheless, even a weak p-state interaction has a significant effect on the effective mass of a nucleon in nuclear matter. The effective mass depends only on β and η, the ratio (apart from sign) of the p-state to s-state interaction strength $-t_2/t_1$, through the combination $\beta(1-1.667\eta)$, but is independent of γ.

On the other hand, the $\rho^{5/3}$ terms in the binding energy of nuclear matter and ^{16}O depend also on γ. They are proportional to

$$0.3\beta(1-1.667\eta)+\gamma \text{ and } 0.380\beta(1-0.762\eta)+\gamma, \tag{32}$$

respectively. Furthermore, in case a p-wave term should indeed be necessary in the effective interaction, it may well have to be repulsive ($\eta < 0$), such as the well-known Rosenfeld interaction. Such an odd-state repulsion seems to be required in order to account for the low energy of the first 0^+ excited state in ^{16}O at 6.06 MeV,[30] and for the α clustering in light nuclei.[31] With a pure s state or a "realistic" interaction, the 0^+ state in ^{16}O is predicted to occur at 15 to 30 MeV, depending on the detailed assumptions made,[32] and the α structure in even-even $N=Z$ light nuclei collapses.[31] Of course, with such an interaction including an odd-state repulsion, it becomes difficult to fit binding energies and rms charge radii, and probably also single-particle energy levels.[33] This point has still to be explored further.

Density Dependence and Spin Dependence of the $\delta(\vec{s})$ Interaction Term

This point was already discussed above.

Three-Body δ vs Density-Dependent Two-Body δ Interaction

The connection between these two interactions was already discussed by VB[3] and by Krieger and Moszkowski.[34] For $N=Z$ nuclei, the effect of the three-body δ interaction, $t_3\delta(\vec{s}_{12})\delta(\vec{s}_{13})$, proposed by Skyrme to simulate the density dependence of the effective interaction (i.e., essentially the G matrix), can be reproduced by a two-body δ interaction $\gamma^1\rho(\vec{r})\delta(\vec{s})$ where $\gamma^1=\frac{1}{6}t_3$ as far as total energy and single-particle energies are concerned. For separation energies there is a slight difference, however, due to a spurious self-interaction term in the two-body interaction.[7,34]

For nuclei with $N\neq Z$, the above equivalence breaks down.[3,34] This can be understood physically if we consider pure neutron matter. The three-body δ interaction leads to vanishing interaction energy (at least two of the neutrons must have the same spin direction, and thus they cannot be at the same point). On the other hand, a two-body δ interaction, even a density-dependent one, gives a finite interaction energy. This difference appears also in the calculation of the asymmetry energy. The contribution of the three-body interaction to the asymmetry energy turns out to be 3 times as large as the contribution of the "equivalent" density-dependent two-body term. (Both contributions are negative; thus, if other things are equal, i.e. for $N=Z$ nuclei, the Skyrme-type interaction leads to more binding for $N\neq Z$ nuclei than the equivalent MDI interaction.)

12. CONCLUSION

This paper deals with HF calculations for double-closed-shell nuclei and the comparison of the re-

sults using the MDI with experiment and calculations of others. Looking at the binding energies, nuclear-charge radii, and single-particle energies revealed that the MDI gives quite satisfactory agreement with experiment for spherical double-closed-shell nuclei.

The MDI with only three arbitrary parameters (apart from spin-orbit coupling which was regarded as a fixed parameter) gives, in general as good results as those using more complicated nuclear interactions, such as the Skyrme interaction as used by VB[3] or the realistic effective interaction introduced by Negele.[10] Due to the simplicity of the MDI, further calculations, such as for deformed nuclei, neutron-star matter (now in progress), and two-particle–two-hole excitations, can be done to study the extent to which this interaction can be used.

ACKNOWLEDGMENTS

The authors are grateful to Professor Chun Wa Wong for valuable comments and suggestions concerning this work. We also wish to thank the University of California at Los Angeles campus computing network for making computing time available on their IBM 360/91.

APPENDIX I

HF Single-Particle Potential for the MDI

We restrict ourselves to the HF potential due to a short-range density-independent interaction $v(s)$ acting only in even states. In the notation of Ref. 2, used here, we consider only the terms in

$$\alpha = -\int v d^3s\,, \quad \beta = -\frac{1}{3}\int v s^2 d^3s\,. \tag{AI1}$$

It was recently shown by Negele and Vautherin[35] that this truncation can also be applied, with slight modification, to realistic nuclear forces, a part of which (e.g. the one-pion exchange interaction) is comparatively long ranged.

The contribution of a density-dependent δ interaction, of strength proportional to $\rho^{2/3}$, to the HF potential is obtained by replacing α by $-\gamma(\frac{3}{2}\pi^2)^{2/3} \times \rho^{2/3}(\vec{\mathbf{r}})$. (There is also an additional rearrangement term discussed in Appendix II.)

The HF potential, U, is defined by the relation $(\text{P.E.})_i = \psi_i^* U \psi_i$, where $(\text{P.E.})_i$ is the potential-energy density associated with a particle in state i. For the direct term of the potential we have

$$U_D\psi_i(\vec{\mathbf{r}}) = \left[\int \rho(\vec{\mathbf{r}}+\vec{\mathbf{s}})v(s)d^3s\right]\psi_i(\vec{\mathbf{r}})\,. \tag{AI2}$$

Expanding the integral in powers of s, and averaging over angle (both ρ and v are assumed to be spherically symmetric), we obtain:

$$U_D = -\alpha\rho - \tfrac{1}{2}\beta\nabla^2\rho\,. \tag{AI3}$$

The calculation of the exchange contribution to the potential is more complicated. We have

$$U_X\psi_i(\vec{\mathbf{r}}) = \sum_j \int \psi_j^*(\vec{\mathbf{r}}+\vec{\mathbf{s}})v(s)\psi_j(\vec{\mathbf{r}})\psi_i(\vec{\mathbf{r}}+\vec{\mathbf{s}})d^3s\,. \tag{AI4}$$

Again we expand the integrand in powers of s and average over angles. This gives

$$U_X\psi_i = -\alpha\rho\psi_i - \tfrac{1}{2}\beta[\rho\nabla^2\psi_i + 2\sum_j(\nabla\psi_j^*\cdot\psi_j)\cdot\nabla\psi_i + \tfrac{1}{2}\sum_j(\nabla^2\psi_j^*\cdot\psi_j)\psi_i + \tfrac{1}{2}\sum_j(\psi_j^*\nabla^2\psi_j)\psi_i]\,. \tag{AI5}$$

Using the equations

$$\sum_j(\psi_j^*\nabla^2\psi_j + \nabla^2\psi_j^*\cdot\psi_j) = \tfrac{1}{2}\nabla^2\rho - 2\tau\,, \tag{AI6}$$

where

$$\tau = \sum_j(\tfrac{1}{2}\nabla\psi_j^*\cdot\nabla\psi_j - \tfrac{1}{4}\psi_j^*\nabla^2\psi_j - \tfrac{1}{4}\nabla^2\psi_j^*\cdot\psi_j) \tag{AI7}$$

and

$$\tfrac{1}{2}\psi_i^*(\rho\nabla^2 + \nabla^2\cdot\rho)\psi_i = \tfrac{1}{2}\psi_i^*\nabla^2\rho\psi_i + \psi_i^*\nabla\rho\cdot\nabla\psi_i + \psi_i^*\rho\nabla^2\psi_i\,. \tag{AI8}$$

We finally obtain the exchange potential

$$U_X = -\alpha\rho - \tfrac{1}{4}\beta(\rho\nabla^2 + \nabla^2\cdot\rho) + \tfrac{1}{8}\beta\nabla^2\rho + \tfrac{1}{2}\beta\tau\,. \tag{AI9}$$

For the MDI, which acts only in even states (in particular, the s state), the HF potential is given by

$$U_{HF} = \tfrac{3}{8}U_D + \tfrac{3}{8}U_X\,. \tag{AI10}$$

This gives Eq. (2) in the text.

The exchange potential can also be written in a more symmetrical form:

$$U_X = -\alpha\rho - \tfrac{1}{8}\beta(\rho\nabla^2 + 2\nabla\cdot\rho\cdot\nabla + \nabla^2\cdot\rho) + \tfrac{1}{2}\beta\tau \tag{AI11}$$

which does not contain the "finite range" term $\nabla^2\rho$. If the interaction contains a p-state term, $\beta\eta\nabla\delta(\vec{\mathbf{s}})\cdot\nabla$, then the total HF potential is

$$U_{HF} = \frac{3+5\eta}{8}U_D + \frac{3-5\eta}{8}U_X\,. \tag{AI12}$$

APPENDIX II

Rearrangement Potential

If an interaction is density-dependent, then there appears a rearrangement potential[7]

$$\langle i\,|\,U_R\,|\,i\rangle = \frac{1}{2}\sum_j\sum_\alpha\left\langle j\,\alpha\left|\psi_i^*\psi_i\frac{dV}{d\rho}\right|j\,\alpha\right\rangle. \tag{AII1}$$

For a density-dependent interaction of the form

$\gamma^1\rho^n(\vec{r})\delta(\vec{s})$ we find:

$$\psi_i^* U_R \psi_i = \gamma^1 \frac{n}{2} \rho^{n-1} \psi_i^* \psi_i \sum_j \sum_\alpha \rho_j \rho_\alpha . \quad \text{(AII2)}$$

The rearrangement potential can be easily obtained:

$$U_R = \gamma^1 \frac{n}{2} \rho^{n-1} (\tfrac{1}{2}\rho_p{}^2 + 2\rho_p \rho_n + \tfrac{1}{2}\rho_n{}^2) . \quad \text{(AII3)}$$

This is the result quoted in Eq. (8) with $n = \frac{2}{3}$. We can define a rearrangement energy

$$E_R = \sum_i \langle i | U_R | i \rangle . \quad \text{(AII4)}$$

Ripka[7] has shown that this E_R has to be subtracted from the HF energy to obtain the total energy:

$$E = \tfrac{1}{2} \sum_i [(\hbar^2/2M)\langle \tau_i \rangle + E_i] - \tfrac{1}{2} E_R . \quad \text{(AII5)}$$

---

*Work partially supported by the National Science Foundation.

†A part of the work described in this paper was done in partial fulfillment of the requirements for a Ph.D. degree.

[1]T. H. R. Skyrme, Phil. Mag. 1, 1043 (1956); Nucl. Phys. 9, 615 (1959).

[2]S. A. Moszkowski, Phys. Rev. C 2, 402 (1970).

[3]D. Vautherin and D. M. Brink, Phys. Letters 32B, 149 (1970); Phys. Rev. C 5, 626 (1972).

[4]H. A. Bethe and R. F. Bacher, Rev. Mod. Phys. 8, 82 (1936).

[5]R. J. Blin-Stoyle, Phil. Mag. 46, 973 (1955); J. S. Bell and T. H. R. Skyrme, *ibid.* 1, 1055 (1956).

[6]D. Vautherin and M. Veneroni, Phys. Letters 26B, 552 (1968).

[7]G. Ripka, lectures given at Duilovo, Yugoslavia, 1969 (unpublished). See also N. E. Reid, M. K. Banerjee, and G. J. Stephenson, Phys. Rev. C 5, 41 (1972).

[8]K. A. Brueckner, J. L. Gammel, and H. Weitzner, Phys. Rev. 110, 431 (1958).

[9]A. M. Green, Nucl. Phys. 33, 218 (1962).

[10]J. W. Negele, Phys. Rev. C 1, 1260 (1970).

[11]L. R. B. Elton, *Nuclear Sizes* (Oxford U. P., London, 1961), p. 31.

[12]A. Bohr and B. R. Mottelson, *Nuclear Structure* (Benjamin, New York, 1969), Vol. 1, p. 237.

[13]A. Bohr and B. R. Mottelson, *Nuclear Structure* (see Ref. 12), p. 271.

[14]G. E. Brown, J. H. Gunn, and P. Gould, Nucl. Phys. 46, 598 (1963).

[15]F. D. Becchetti, Jr., and G. W. Greenlees, Phys. Rev. 182, 1190 (1969).

[16]W. D. Myers and W. J. Swiatecki, Nucl. Phys. 81, 1 (1966).

[17]P. J. Siemens, Nucl. Phys. A141, 225 (1970).

[18]K. A. Brueckner and J. Dabrowski, Phys. Rev. 134, B722 (1964).

[19]F. G. Perey, Phys. Rev. 131, 745 (1963).

[20]We are grateful to Dr. C. Dover for pointing this out to us.

[21]J. Németh and D. Vautherin, Phys. Letters 32B, 561 (1970).

[22]H. S. Köhler, Nucl. Phys. A170, 88 (1971).

[23]L. D. Miller and A. E. S. Green, Phys. Rev. C 5, 241 (1972).

[24]J. H. E. Mattauch, W. Thiele, and A. H. Wapstra, Nucl. Phys. 67, 1 (1965).

[25]H. R. Collard, L. R. B. Elton, and R. Hofstadter, in *Landolt-Börnstein Numerical Data and Functional Relationships in Science and Technology*, edited by K. H. Hellwege and H. Schopper (Springer-Verlag, Berlin, Germany, 1967), New Series, Group I, Vol. 2, Chap. 2, Sec. 2, p. 1.

[26]R. E. Frosch *et al.*, Phys. Rev. 174, 1380 (1968); J. Heisenberg *et al.*, Phys. Rev. Letters 23, 1402 (1969).

[27]See Refs. 3 and 10; A. Faessler *et al.*, Nuovo Cimento (to be published); J. Németh and G. Ripka, private communication.

[28]G. R. Satchler, in *Isospin in Nuclear Physics*, edited by D. Wilkinson (North-Holland, Amsterdam, 1969), Chap. 9.

[29]C. J. Batty, E. Friedman, and C. W. Greenlees, Nucl. Phys. A127, 368 (1969); J. Zimanyi and B. Gyarmati, Phys. Rev. 174, 1112 (1968).

[30]W. H. Bassichis and G. Ripka, Phys. Letters 15, 320 (1965).

[31]S. B. Khadkikar, Phys. Letters 36B, 451 (1971).

[32]S. J. Krieger, Phys. Rev. Letters 22, 97 (1969).

[33]D. M. Brink and E. Boeker, Nucl. Phys. A91, 1 (1967).

[34]S. J. Krieger and S. A. Moszkowski, Phys. Rev. C 5, 1990 (1972).

[35]J. W. Negele and D. Vautherin, Phys. Rev. C 5, 1472 (1972).

[36]H. A. Bethe, Ann. Rev. Nucl. Sci. 21, 93 (1971).